

DMD 14894

Effect of silibinin on the pharmacokinetics of pyrazinamide and pyrazinoic acid in rats

Jhy-Wen Wu, Tung-Hu Tsai

Institute of Traditional Medicine, School of Medicine, National Yang-Ming University, Taipei 112, Taiwan (J.W.W., T.H.T.); Centers for Disease Control, Department of Health, Taipei, Taiwan (J.W.W.); Department of Medical Research and Education, Taipei Veterans General Hospital, Taipei, Taiwan (T.H.T.); and Department of Education and Research, Ren-Ai Branch, Taipei City Hospital, Taipei, Taiwan (T.H.T.)

DMD 14894

Running title: Effect of silibinin on the pharmacokinetics of pyrazinamide

Author for correspondence:

Tung-Hu Tsai, Ph.D.

Professor

National Yang-Ming University, School of Medicine,

Institute of Traditional Medicine

155, Li-Nong Street Section 2

Taipei 112, Taiwan

Telephone: (886-2) 2826-7115; Fax: (886-2) 2822-5044

E-mail: thtsai@ym.edu.tw

Number of text pages: 18

Number of tables: 3

Number of figures: 10

Number of references: 34

Number of words in Abstract: 224

Number of words in Introduction: 600

Number of words in Discussion: 1013

non-standard abbreviations: ACD, anticoagulant citrate dextrose; AUC, area under the concentration versus time curve; Cl, clearance; C_{\max} , maximum concentration; PZA, pyrazinamide; PA, pyrazinoic acid; TB, tuberculosis; $t_{1/2}$, elimination half-life.

DMD 14894

Abstract

Pyrazinamide (PZA) is widely used in combination with other drugs in chemotherapy for tuberculosis (TB). However, the dose-related liver injury is the main adverse effect of PZA and its metabolite (pyrazinoic acid; PA). Silibinin is the main flavonoid extracted from milk thistle (*Silybum marianum*), and it displays hepatoprotective properties. This study investigates the pharmacokinetics of PZA and PA, and their interaction with silibinin in rats. The parallel study design was divided into six groups: PZA alone, PZA + long-term silibinin exposure, PZA + concomitant short-term silibinin exposure, PA alone, PA + long-term silibinin exposure, and PA + concomitant short-term silibinin exposure groups. The results indicate that the distribution ratio of PZA from bile-to-blood ($AUC_{\text{bile}}/AUC_{\text{blood}}$) in the PZA + long-term silibinin exposure and PZA + concomitant short-term silibinin exposure groups was also not significantly different when compared with the PZA alone group. However, the bile-to-blood distribution ratio of PA was significantly decreased from the PA + long-term silibinin exposure and the PA + concomitant short-term silibinin exposure groups. Upon PZA administration, the blood but not bile levels of PA were markedly increased in the PZA + long-term silibinin exposure and PZA + concomitant short-term silibinin exposure groups but the bile-to-blood ratio of PA was decreased. These results suggest that the excretion pathway of PA might be blocked by silibinin through xanthine oxidase and hepatobiliary excretion.

DMD 14894

Introduction

Pyrazinamide is one of the frontline agents prescribed for the treatment of *Mycobacterium tuberculosis*. It is considered to be a prodrug of PA, which is believed to be the active inhibitor of *M. tuberculosis* (Trnka et al., 1964). However, PZA has some drawbacks since it is associated with liver dysfunction (Singh et al., 1995; Kunimoto et al., 2003; Yee et al., 2003) and with hyperuricemia (Lacroix et al., 1988; Solangi et al., 2004). PA is the main active metabolite of PZA, which is produced by the liver microsomal deamidase and then PA is further hydroxylated to 5-hydroxypyrazinoic acid (5-hydroxy-PA), by xanthine oxidase. The other metabolic pathway, PZA is directly oxidized to 5-hydroxypyrazinamide (5-hydroxy-PZA) by xanthine oxidase. These three metabolites of PZA are mainly excreted in urine. One minor part of PZA metabolic pathway consists of PA with glycine to give pyrazinuric acid (Lacroix et al., 1988). Some drugs, like silibinin, could be a challenger to compete with the two hydroxylated metabolites for glucuronidation.

Silymarin, which contains polyphenolic flavonoids, is extracted from the seeds of milk thistle (*Silybum marianum*), has been used for its hepatoprotective effects in clinical application (Flora et al., 1998). Derivatives of milk thistle have been used as herbal remedies for a long time; silibinin is the main flavonolignan of silymarin, with stereoisomers such as isosilybin, dihydrosilybin, silydianin, and silychristin (Wagner et al., 1968; Wagner et al., 1974). It displays hepatoprotective properties and can be used clinically for the treatment of toxic liver damage and chronic liver disease. The protective effects of silymarin have been studied in various models of experimental liver damage (Valenzuela et al., 1985; Mourelle et al., 1989; Muriel et al., 1992).

DMD 14894

Silymarin appears to enhance the recovery from hepatic damage induced by antitubercular drugs (Tasduq et al., 2005).

Results of clinical trials suggest that silymarin might be more effective than a placebo for viral hepatitis and for hepatitis caused by toxins and alcohol (Flora et al., 1998; Pepping, 1999). Silymarin has also been reported to prevent liver damage caused by a variety of drugs, including phenytoin, halothane and phenothiazines (Pepping, 1999). However, little is known about the drug interaction potential of silymarin. A clinical study has indicated that silymarin might induce both intestinal P-glycoprotein and CYP3A4 upon multiple dose administration (Rajnarayana et al., 2004). The in vitro studies have suggested an inhibitory effect on the xanthine oxidase (Sheu et al., 1998), which is responsible for the metabolism of PZA.

Herbal remedies and complementary medicines are widely used, despite a lack of information about their pharmacology, pharmacokinetics, and potential drug-drug interaction. The incidence of PZA-induced hepatotoxicity during treatment for active tuberculosis (TB) is substantially higher than that with other first-line anti-TB drugs (Yee et al., 2003), and silymarin is used as a therapeutic agent for many types of acute and chronic liver diseases (Flora et al., 1998). TB meningitis is one of the most devastating infectious diseases involving the central nervous system, and the drugs containing PZA is generally advised for the treatment of TB meningitis (van Loenhout-Rooyackers et al., 2001). Barzaghi et al., (1990) demonstrates that the Pharmacokinetics of human subjects shows a pattern similar to rats. In this study, we describe the pharmacokinetics of PZA and PA alone as the control groups, and the effects of long-term silibinin exposure and concomitant short-term silibinin exposure

DMD 14894

groups in rats. In addition, we show that the hepatobiliary distribution of PA was inhibited by silibinin, but not its parent drug PZA. The brain-to-blood ($AUC_{\text{brain}}/AUC_{\text{blood}}$) distribution ratio of PZA will be investigated in this study. The bile-to-blood ($AUC_{\text{bile}}/AUC_{\text{blood}}$) distribution ratio of PA was decreased after silibinin exposure.

Methods

Experimental animals

All experimental protocols involving animals were reviewed and approved by the institutional animal experimentation committee of the National Yang-Ming University. Male specific pathogen-free Sprague-Dawley rats weighing 280-320 g were obtained from the Laboratory Animal Center of the National Yang-Ming University. The animals had free access to food (Laboratory Rodent Diet 5001, PMI Feeds Inc., Richmond, IN, USA) and water until 18 h prior to being used in experiments, and after that only food was removed. The rats were initially anesthetized with urethane 1 g ml⁻¹ and α -chloralose 0.1 g ml⁻¹ (1 ml kg⁻¹, i.p.), and remained anesthetized throughout the microdialysis sampling period. The femoral vein was exposed for further drug administration. The rat's body temperature was maintained at 37 °C with a heating pad during the experiment.

Chemicals and Reagents

PZA, PA and silibinin were purchased from Sigma Chemicals (St. Louis, MO, USA). Liquid chromatographic grade solvents and reagents were obtained from E. Merck (Darmstadt, Germany). Triply de-ionized water from Millipore (Bedford, MA, USA)

DMD 14894

was used for all preparations.

Liquid Chromatography

The HPLC system consisted of a chromatographic pump (BAS PM-80, West Lafayette, IN, USA), an off-line fraction collector (CMA 140, Stockholm, Sweden) equipped with a 20 μ l sample loop, and an ultraviolet detector (Varian, Walnut Creek, CA, USA). PZA, PA and dialysate were separated using an Alltech, Altima C18 column (150 x 4.6 mm i.d.; particle size 5 μ m) maintained at 30 °C. The mobile phase comprised of 10 mM monosodium phosphate – triethylamine (100:0.1, v/v, pH 3 adjusted by orthophosphoric acid), and the flow rate of the mobile phase was 1 ml min^{-1} . The mobile phase was filtered through a Millipore 0.45 μ m filter and degassed prior to use. The optimal UV detection for PZA and PA was set at a wavelength of 268 nm. Output data from the detector were integrated via an EZChrom chromatographic data system (Scientific Software, San Ramon, CA, USA).

Method validation

The intra-day and inter-day variabilities for PZA and PA were assayed (six replicates) at concentrations of 0.1, 0.5, 1, 5, 10, 50 and 100 $\mu\text{g ml}^{-1}$ on the same day and on six sequential days, respectively. The accuracy (% Bias) was calculated from the nominal concentration (C_{nom}) and the mean value of observed concentration (C_{obs}) as follows: $\text{Bias (\%)} = [(C_{\text{obs}} - C_{\text{nom}}) / (C_{\text{nom}})] \times 100$. The precision relative standard deviation (RSD) was calculated from the observed concentrations as follows: $\% \text{ RSD} = [\text{standard deviation (SD)} / C_{\text{obs}}] \times 100$. Accuracy (% Bias) and precision (% RSD) values of the limit of the quantification was pre-defined within $\pm 15\%$ (Bressolle et al., 1996). The limit of quantification served as the lowest concentration of calibration curve.

DMD 14894

Microdialysis experiment

Blood, brain and bile microdialysis systems each consisted of a microinjection pump (CMA/100, Stockholm, Sweden), microdialysis probes and stereotaxic frame. The dialysis probes for blood (10 mm in length), brain (3 mm in length) and bile (7 cm in length) were made of silica capillary in a concentric design with their tips covered by the dialysis membrane (Spectrum, 150 mm outer diameter with a cut-off at nominal molecular mass of 13,000, Laguna Hills, CA, USA). The blood microdialysis probe was positioned within the jugular vein toward the right atrium and then perfused with anticoagulant citrate dextrose and ACD solution (citric acid 3.5 mM; sodium citrate 7.5 mM; dextrose 13.6 mM) at a flow-rate of $2.4 \mu\text{l min}^{-1}$.

The bile duct microdialysis probe was constructed in our own laboratory (Tsai, 2001; Tsai et al., 2001) based on the design originally described by Scott and Lunte (Scott and Lunte, 1993). A 7-cm dialysis membrane was inserted into the polyethylene tubing (PE-60; 0.76 mm I.D. x 1.22 mm O.D., Clay-Adams, NJ, USA). The ends of the dialysis membrane and PE-60 were inserted into the silica tubing (40 mm I.D x 140 mm O.D., SGE, Australia) and PE-10 (0.28 mm I.D. x 0.61 mm O.D.), respectively. Both ends of the tubing and the union were cemented with epoxy and the epoxy was allowed to dry for at least 24 h. For post bile duct cannulation, the microdialysis probe was then perfused with Ringer's solution (147 mM Na^+ ; 2.2 mM Ca^{2+} ; 4 mM K^+ ; pH 7.0) at $2.4 \mu\text{l min}^{-1}$ flow rate.

After the implantation of blood and bile microdialysis probes, each rat was

DMD 14894

immobilized in a stereotaxic frame (David Kopf Instruments, Tujunga, CA, USA). The skull was surgically exposed, and a hole was trephined into the skull based on stereotaxic coordinates. The brain microdialysis probe was placed into the right striatum (0.2 mm anterior to bregma, 3.2 mm lateral to midline and 7.5 mm lower to tip). The brain microdialysis probe was perfused with Ringer's solution at a flow-rate of $2.4 \mu\text{l min}^{-1}$.

Drug administration

Animals were divided into six groups, after a 2 h post-surgical stabilization period following the implantation of microdialysis probes, PZA (50 mg kg^{-1} , i.v.) or PA (30 mg kg^{-1} , i.v.) was administered via the femoral vein as the control groups of PZA alone and PA alone groups, respectively. The following four treated groups were PZA + long-term silibinin exposure, PA + long-term silibinin exposure, PZA + concomitant short-term silibinin exposure, and PA + concomitant short-term silibinin exposure group.

For the PZA + long-term silibinin exposure group and PA + long-term silibinin exposure group, silibinin 100 mg kg^{-1} was given orally for three consecutive days and on the fourth day, PZA (50 mg kg^{-1} , i.v.) or PA (30 mg kg^{-1} , i.v.) was administered via the femoral vein, respectively. For the PZA + concomitant short-term silibinin exposure group or PA + concomitant short-term silibinin exposure group, silibinin (30 mg kg^{-1}) was injected via femoral vein 10 min prior to PZA (50 mg kg^{-1} i.v.) or PA (30 mg kg^{-1} , i.v.), respectively. Dialysates were collected from the blood, brain and bile by a fraction collector (CMA/140) at 10 min intervals and immediately analyzed by a

DMD 14894

refrigerated microsampler (CMA/200) coupled to a validated HPLC system.

Recovery of microdialysate

It is possible that the analytes adhere to the microdialysis apparatus. Besides, matrix effect and cross over could disturb the microdialysis and analytical systems. To avoid these interferences, an in vivo recovery was performed by the following steps. The blood, brain and bile microdialysis probes were inserted into the rat jugular vein, brain striatum and bile duct under anesthesia with urethane 1 g ml⁻¹ and chloralose 0.1 g ml⁻¹. Ringer's solutions containing PA 6, 10 and 20 µg ml⁻¹, and PZA 10, 30 and 60 µg ml⁻¹ were passed through the microdialysis probe into rat bile and brain. In addition, ACD solutions containing PA 6, 10 and 20 µg ml⁻¹, and PZA 10, 30 and 60 µg ml⁻¹ were passed through the microdialysis probe into rat blood. These were all done by individual experiment at a constant flow rate of 2.4 µl min⁻¹ using an infusion pump (CMA 100). Following a stabilization period of 2 h post probe implantation, the perfusate (C_{perf}) and dialysate (C_{dial}) concentrations of PZA and PA were determined by HPLC. The in vivo relative recovery (R_{dial}) of PZA and PA across the microdialysis probe was calculated by the following equation: $R_{\text{dial}} = (C_{\text{perf}} - C_{\text{dial}})/C_{\text{perf}}$.

Pharmacokinetic application

The protein-unbound concentrations (C_u) of analytes in the extracellular fluid were corrected from the concentration in dialysate (C_m) as follows: $C_u = C_m/R_{\text{dial}}$. Pharmacokinetic calculations were performed on each individual set of data using the pharmacokinetic software WinNonlin Standard Edition Version 1.1 (Pharsight Corp.,

DMD 14894

Mountain View, CA, USA) by the noncompartmental method.

The areas under the concentration-time curves (AUC) were calculated according to the log linear trapezoidal method. The clearances (Cl) were calculated as follows: $Cl = \text{dose}/AUC$. The blood to tissue distributions were calculated as follows: $AUC_{\text{tissue}}/AUC_{\text{blood}}$ (Lin et al., 1982). All data are presented as mean \pm standard error mean.

Statistics

The results were represented as mean \pm standard error of the mean. The statistical analysis was performed with SPSS version 10.0 (SPSS Inc. Chicago, IL, USA). One-way ANOVA was followed by a Dunnett's post hoc test comparison among PZA alone, PZA + long-term silibinin exposure and PZA + concomitant short-term silibinin exposure groups, and PA alone, PA + long-term silibinin exposure and PA + concomitant short-term silibinin exposure groups. All statistical tests were performed at the two-sided 5% level of significance.

Results

Chromatograms in blood, brain and bile

The characteristics of analytes are hydrophilic compounds and the mobile phase without contain organic solvent for the reversed phase column. In order to avoid the contamination of endogenous substance or analytes in the column, the column was washed with methanol (50%) for 1 hr after experimental day. Following the above method, protein-unbound PZA was found in the dialysates of blood, brain and bile,

DMD 14894

while the PA metabolite was found in the dialysates of blood and bile. This result suggests that PA was undetectable in the brain dialysis. Typical chromatograms of PZA and PA in rat blood dialysates are shown in Figure 1. Separation of PZA and PA from endogenous substances in the blood dialysate was achieved in an optimal mobile phase containing 10 mM monosodium phosphate – triethylamine (100:0.1, v/v, pH 3 adjusted by orthophosphoric acid). The retention times of PA and PZA were 7 and 12 min, respectively. Figure 1A shows a calibration sample of PZA ($10 \mu\text{g ml}^{-1}$) and PA ($10 \mu\text{g ml}^{-1}$), and Figure 1B shows the chromatogram of a blank blood dialysate. None of the observed peaks interfered with the analyte within the retention times of the analytes. Figure 1C shows the chromatogram of a blood dialysate sample containing PA ($0.45 \mu\text{g ml}^{-1}$) and PZA ($19.22 \mu\text{g ml}^{-1}$) collected from the rat blood microdialysate at 90 min after PZA administration (50 mg kg^{-1} , i.v.).

Figure 2A shows a calibration sample of PA ($5 \mu\text{g ml}^{-1}$) and PZA ($5 \mu\text{g ml}^{-1}$), and Figure 2B shows the chromatogram of a blank brain dialysate. Figure 2C shows the chromatogram of a brain dialysate sample containing PZA ($4.26 \mu\text{g ml}^{-1}$) collected from the rat brain microdialysate 40 min post PZA administration (50 mg kg^{-1} , i.v.). PA in brain dialysate was not detected in this analytical system.

Figure 3A shows a calibration sample of standard PA ($10 \mu\text{g ml}^{-1}$) and PZA ($10 \mu\text{g ml}^{-1}$). Figure 3B shows the chromatogram of a blank bile dialysate sample obtained from bile duct microdialysis probe before the drug administration. Figure 3C shows the chromatogram of bile dialysate sample containing PA ($1.07 \mu\text{g ml}^{-1}$) and PZA ($12.22 \mu\text{g ml}^{-1}$) collected from the rat bile microdialysate 200 min post PZA administration (50 mg kg^{-1} , i.v.). To avoid the interference of endogenous peak, the

DMD 14894

small amount of peak area was calculated by valley-to-valley.

Method validation

The calibration curves of PZA and PA were obtained prior to the LC analysis of dialysates over a concentration range of 0.1–100 $\mu\text{g ml}^{-1}$ ($r^2 > 0.995$). The concentrations of PZA and PA were linearly related to the peak areas of the chromatogram. The intra-assay and inter-assay accuracy and precision were thus found to be acceptable for the analysis of a dialysis sample in support of pharmacokinetic studies (Bressolle et al., 1996). This method is sufficiently sensitive to allow for the measurement of PA in rat blood, bile and PZA in rat blood, brain and bile for pharmacokinetic study.

In vivo recoveries of PA and PZA

Average in vivo recoveries of PZA were $33.4 \pm 1.7 \%$, $15.4 \pm 0.9 \%$ and $80.3 \pm 1.6 \%$ for blood, brain and bile, respectively. Average in vivo recoveries of PA were $36.0 \pm 1.8 \%$, $16.3 \pm 0.8 \%$ and $81.9 \pm 1.5 \%$ for blood, brain and bile, respectively. The data indicated that no significant difference in recovery values for the same region was observed after the addition of PZA or PA to the perfusate. The recoveries from the microdialysis probes in rat blood, brain and bile were independent of the concentration required for these experiments. The surface area of the dialysis membrane is one of the major factors for the recovery. Due to the small brain regional area, the dialysis membrane of microdialysis probe is much smaller than the probes for blood and bile. This may lead to the brain recovery smaller than the blood and bile.

DMD 14894

Interaction of silibinin and protein-unbound PZA in blood, brain and bile

Figures 4-8 show PZA and its metabolite PA concentrations versus time profiles in blood, brain and bile for the PZA alone, PZA + long-term silibinin exposure and PZA + concomitant short-term silibinin exposure groups, respectively. Pharmacokinetic data for PZA and PA are presented in Tables 1-2. The pharmacokinetic curves for the group of PZA alone reflect the fact that the disposition of PZA in rat bile exhibited a peak concentration at 20 min after PZA administration (50 mg kg^{-1}), followed by a slow elimination phase.

For the groups of PZA alone, PZA + long-term silibinin exposure and PZA + concomitant short-term silibinin exposure, PZA concentrations in the blood were not significantly altered. The metabolite PA concentrations in blood were gradually increased after PZA administration up to a plateau during 1-2 h (Fig. 5). The blood AUCs of PZA in both PZA + long-term silibinin exposure group and PZA + concomitant short-term silibinin exposure groups were 18200 ± 4500 and $20200 \pm 2100 \text{ min } \mu\text{g ml}^{-1}$, which was not significantly different from the PZA alone group (19300 ± 3800). However, the AUCs of metabolite PA in both PZA + long-term silibinin exposure and PZA + concomitant short-term silibinin exposure groups were 809 ± 69 and $568 \pm 23 \text{ min } \mu\text{g ml}^{-1}$, which were significantly higher than the PZA alone group (212 ± 22).

After long-term silibinin exposure or concomitant short-term silibinin exposure prior to PZA administration, PZA concentrations in the brain were not significantly altered (Fig. 6). The brain AUCs of PZA in the groups of PZA + long-term silibinin exposure and PZA + concomitant short-term silibinin exposure were 6900 ± 710 and $7800 \pm$

DMD 14894

880 min $\mu\text{g ml}^{-1}$, which were not significantly different from the PZA alone group (7900 ± 1700 min $\mu\text{g ml}^{-1}$).

After long-term silibinin exposure or concomitant short-term silibinin exposure prior to PZA administration, the PZA concentrations in bile were not significantly altered (Fig. 7). The bile AUCs of PZA in both groups of PZA + long-term silibinin exposure and PZA + concomitant short-term silibinin exposure were 14900 ± 2300 and 23900 ± 3600 min $\mu\text{g ml}^{-1}$, which were not significantly different from the PZA alone group (20500 ± 4200). The metabolite PA concentrations in bile were gradually increased after PZA administration up to a plateau around 1 h (Fig. 8). The AUCs of the metabolite PA in both groups PZA + long-term silibinin exposure and PZA + concomitant short-term silibinin exposure were 649 ± 29 and 407 ± 76 min $\mu\text{g ml}^{-1}$, respectively, which were not significantly different from the PZA alone group (527 ± 28 min $\mu\text{g ml}^{-1}$).

The hepatobiliary distribution of PZA was defined as the bile-to-blood distribution (k value), which was calculated by the AUC ratio in bile-to-blood ($k = \text{AUC}_{\text{bile}}/\text{AUC}_{\text{blood}}$) (de Lange et al., 1997). The bile-to-blood distribution PZA in both groups of PZA + long-term silibinin exposure and PZA + concomitant short-term silibinin exposure were 0.67 ± 0.10 and 0.96 ± 0.16 , respectively, which were not significantly different from the PZA alone group (1.02 ± 0.16). The brain-to-blood distribution of PZA in both groups of PZA + long-term silibinin exposure and PZA + concomitant short-term silibinin exposure were 0.44 ± 0.12 and 0.40 ± 0.08 , respectively, which were not significantly different from the PZA alone group (0.42 ± 0.05). The bile-to-blood distribution of PA in both groups of PZA + long-term silibinin exposure and PZA +

DMD 14894

concomitant short-term silibinin exposure were 0.81 ± 0.02 and 0.80 ± 0.07 , which were significantly decreased from the PZA alone group (2.67 ± 0.63).

Interaction of silibinin and protein-unbound PA in blood, and bile

Mean PA concentrations versus time profiles in blood, and bile with the PA alone, PA + long-term silibinin exposure and PA + concomitant short-term silibinin exposure groups are presented in Figs. 9-10 and the pharmacokinetic data is presented in Table 3. The pharmacokinetic curves of the PA alone group show that the disposition of PA in rat bile exhibited a peak concentration at 20 min of PA administration (30 mg kg^{-1}), followed by a slow elimination phase.

After long-term silibinin exposure or concomitant short-term silibinin exposure prior to PA administration, PA concentrations in the blood were markedly increased (Fig. 9). The blood AUC of PA in the groups of PA + long-term silibinin exposure and PA + concomitant short-term silibinin exposure groups were 3140 ± 300 and $3730 \pm 380 \text{ min } \mu\text{g ml}^{-1}$, which was significantly increased from the PA alone group (892 ± 140) (Table 3).

The PA concentrations in the bile quickly reached a maximum level within 20 min and then gradually decreased (Fig. 10). After concomitant short-term silibinin exposure prior to PA administration, PA concentrations in the bile were not significantly altered, but after long-term silibinin exposure, PA concentrations in the bile were significantly decreased. The bile AUC of PA in the PA + long-term silibinin exposure groups were 2830 ± 270 , which was significantly increased from the PA alone group. The bile AUC of PA in the PA + concomitant short-term silibinin

DMD 14894

exposure group was $3610 \pm 410 \text{ min } \mu\text{g ml}^{-1}$, which was not significantly different from the PA alone group ($3670 \pm 190 \text{ min } \mu\text{g ml}^{-1}$).

The bile-to-blood excretion PA in the groups of PA + long-term silibinin exposure and PA + concomitant short-term silibinin exposure were 0.96 ± 0.16 and 0.92 ± 0.08 , respectively, which were significantly decreased from the PA alone group (3.74 ± 0.41).

Discussion

This study performed in rats demonstrates that the mean concentration of PZA in the brain increased during the first 10 min, reaching a peak concentration (C_{max} : $23.68 \pm 3.68 \mu\text{g ml}^{-1}$) at 20-30 min (Table 1) of exposure. The minimum inhibitory concentration (MIC) of PZA has been demonstrated at $15 \mu\text{g ml}^{-1}$ for some strain of *M. tuberculosis* at a pH of 5.6 (Heifets et al., 1989). This protein-unbound concentration ranges can be reachable within 300 min after PZA administration at a dosage of 50 mg kg^{-1} , i.v., and these concentration levels were not significantly different in the groups of PZA + long-term silibinin exposure and PZA + concomitant short-term silibinin exposure (Figure 4).

PZA is largely converted to PA and 5-hydroxy-PA, which are subsequently cleared through renal and nonrenal (Stottmeier et al., 1968), with 3% of the dose that appeared unchanged in the urine, and 40% that was excreted as PA (Ellard and Haslam, 1976; Bareggi et al., 1987). The effect of silibinin on PZA level may be counteracted by other PZA biotransformation pathways. After long-term silibinin

DMD 14894

exposure or concomitant short-term silibinin exposure, PZA levels in blood, brain and bile were not significantly different from the PZA alone group.

After PZA administration, the PZA kinetics was unaltered by the associated silibinin, but the AUC of the metabolite PA in the blood of the PZA + long-term silibinin exposure and PZA + concomitant short-term silibinin exposure groups were clearly increased by 382% and 268%, respectively. The silymarin group displayed inhibitory effects on xanthine oxidase (IC_{50} of $27.58 \pm 3.48 \mu\text{M}$) (Sheu et al., 1998), and the possible mechanisms for this interaction include the inhibitory xanthine oxidase and the decrease in hepatobiliary excretion by silibinin. Silibinin may inhibit PZA metabolism to 5-hydroxy-PZA or 5-hydroxy-PA, but PZA passable enzymatic deamidation, followed by the formation of main active metabolite PA. This result is consistent with that reported by Lacroix et al. (1988) for the interaction between allopurinol, a xanthine oxidase inhibitor, and PZA. Drugs affecting xanthine oxidase activity, such as allopurinol or caffeine, significantly affected the PZA metabolism (Lacroix et al., 1988; Mehmedagic et al., 2002). Our study demonstrates that the distribution ratio of PZA from bile-to-blood in the PZA + long-term silibinin exposure and PZA + concomitant short-term silibinin exposure group were not significantly different from the PZA alone group (Table 1). However, the biliary distribution ratio of the metabolite PA was significantly decreased (Table 2). Silibinin did not markedly affect the hepatobiliary distribution of PZA but increased the blood level of PA and markedly affected the hepatobiliary distribution of PA.

Recent clinical study proves that a commercial silibinin formulation was oral administration in prostate cancer patients. The plasma C_{max} concentration of silibinin

DMD 14894

in a patient was greater than the IC_{50} ($27 \mu\text{M}$; $13 \mu\text{g ml}^{-1}$) of xanthine oxidase at daily doses of 13, 15 and 20 g in three divided doses, and the result appears to be good for the treatment of prostate cancer (Flaig et al., 2007). Besides, unpublished data in our laboratory shows that the C_{max} of silibinin in rat plasma was $92 \pm 7 \mu\text{g ml}^{-1}$ (about $190 \mu\text{M}$) after silibinin administration (30 mg kg^{-1} , i.v.). For silibinin tissue distribution in a mouse at an oral dose of 50 mg kg^{-1} , the peak levels of silibinin at 30 min in the liver, lung, stomach, and pancreas were 8.8 ± 1.6 , 4.3 ± 0.8 , 123 ± 21 , and $5.8 \pm 1.1 \mu\text{g g}^{-1}$, respectively. Other tissues retained it for a long time. The peak levels of silibinin at 60 min in the skin and prostate were 1.4 ± 0.5 and $2.5 \pm 0.4 \mu\text{g g}^{-1}$, respectively (Zhao and Agarwal, 1999). The above pharmacokinetic data indicate that the IC_{50} of silibinin on xanthine oxidase should be feasible in an appropriate dose regimens.

Concentrations of PA in the bile higher than those in blood were against a concentration gradient at the dosages of 30 mg kg^{-1} over the same period of time. As seen in Figs. 9-10, the time course of PA levels in bile was greater than those in blood, indicating that PA is condensed in the bile by an active transport excretion or by the formation of micelles in the bile. Active biliary excretion would be compatible with the significantly superior AUC of PA in the bile than that in blood.

In order to find the hepatobiliary distribution pathway of PZA and PA, PA was individually given but not measured by the metabolite of PZA. After PA administration, the hepatobiliary distribution ratio of PA in the PA + long-term silibinin exposure and PA + concomitant short-term silibinin exposure group were 0.96 ± 0.16 and 0.92 ± 0.08 , respectively, which were significantly decreased from the

DMD 14894

PA alone group (3.74 ± 0.41) (Table 3). These data suggest that the hepatobiliary distribution of PA might be excreted through a different process. PA might be blocked by silibinin through xanthine oxidase and there could be a decrease in PA transport into bile. The bile-to-blood ratio of PZA was not significantly different, although the hepatobiliary distribution ratio of PA was decreased on both groups of the metabolite of PZA (Table 2) and PA administered (Table 3).

Apart from hepatic toxicity, hyperuricemia is a common finding in patients treated with PZA (Shapiro and Hyde, 1957; Snider et al., 1984). Silibinin increased the blood concentrations of PA, which is directly responsible for the inhibition of renal urate secretion (Weiner and Tinker, 1972; Ellard and Haslam, 1976). Silibinin displays inhibiting xanthine oxidase in relation with uric acid generation. To determine whether silibinin increase the risks of PZA induce hyperuricemia, must to go a step further study. Out data supported that the metabolic interaction of silibinin and PZA.

In conclusion, the blood, brain and bile pharmacokinetic data presented here are important in confirming the expectation that PZA is rapidly and readily distributed into the bile and brain. Furthermore, the addition of silibinin shows no significant effects on the pharmacokinetic parameters of PZA but shows significant effects on the distribution ratios of PA. These results suggest that the hepatobiliary elimination of PA may be affected by silibinin in the groups of long-term silibinin exposure and concomitant short-term silibinin exposure.

Acknowledgements

We thank Prof. Lie-Chwen Lin, head of the Department of Herbal Medicine, National

DMD 14894

Research Institute of Chinese Medicine, Taipei, Taiwan for her collaboration.

DMD 14894

References

- Bareggi SR, Cerutti R, Pirola R, Riva R and Cisternino M (1987) Clinical pharmacokinetics and metabolism of pyrazinamide in healthy volunteers. *Arzneimittelforschung* **37**:849-854.
- Barzaghi N, Crema F, Gatti G, Pifferi G and Perucca E (1990) Pharmacokinetic studies on IdB 1016, a silybin phosphatidylcholine complex, in healthy human subjects. *Eur J Drug Metab Pharmacokinet* 1990;**15**:333-338.
- Bressolle F, Bromet-Petit M and Audran M (1996) Validation of liquid chromatographic and gas chromatographic methods. Applications to pharmacokinetics. *J Chromatogr B* **686**:3-10.
- de Lange EC, Danhof M, de Boer AG and Breimer DD (1997) Methodological considerations of intracerebral microdialysis in pharmacokinetic studies on drug transport across the blood-brain barrier. *Brain Res Rev* **25**:27-49.
- Ellard GA and Haslam RM (1976) Observations on the reduction of the renal elimination of urate in man caused by the administration of pyrazinamide. *Tubercle* **57**:97-103.
- Flaig TW, Gustafson DL, Su LJ, Zirrolli JA, Crighton F, Harrison GS, Pierson AS, Agarwal R and Glode LM (2007) A phase I and pharmacokinetic study of silybin-phytosome in prostate cancer patients. *Invest New Drugs* **25**:139-146.
- Flora K, Hahn M, Rosen H and Benner K (1998) Milk thistle (*Silybum marianum*) for the therapy of liver disease. *Am J Gastroenterol* **93**:139-143.
- Heifets LB, Flory MA and Lindholm-Levy PJ (1989) Does pyrazinoic acid as an active moiety of pyrazinamide have specific activity against *Mycobacterium tuberculosis*? *Antimicrob Agent Chemother* **33**:1252-1254.

DMD 14894

- Kunimoto D, Warman A, Beckon A, Doering D and Melenka L (2003) Severe hepatotoxicity associated with rifampin-pyrazinamide preventative therapy requiring transplantation in an individual at low risk for hepatotoxicity. *Clin Infect Dis* **36**:e158-161.
- Lacroix C, Guyonnaud C, Chaou M, Duwoos H and Lafont O (1988) Interaction between allopurinol and pyrazinamide. *Eur Respir J* **1**:807-811.
- Lin JH, Sugiyama Y, Awazu S and Hanano M (1982) In vitro and in vivo evaluation of the tissue-to-blood partition coefficient for physiological pharmacokinetic models. *J Pharmacokinetic Biopharm* **10**:637-647.
- Mehmedagic A, Verite P, Menager S, Tharasse C, Chabenat C, Andre D and Lafont O (2002) Investigation of the effects of concomitant caffeine administration on the metabolic disposition of pyrazinamide in rats. *Biopharm Drug Dispos* **23**:191-195.
- Mourelle M, Muriel P, Favari L and Franco T (1989) Prevention of CCL4-induced liver cirrhosis by silymarin. *Fundam Clin Pharmacol* **3**:183-191.
- Muriel P, Garciapina T, Perez-Alvarez V and Mourelle M (1992) Silymarin protects against paracetamol-induced lipid peroxidation and liver damage. *J Appl Toxicol* **12**:439-442.
- Pepping J (1999) Milk thistle: *Silybum marianum*. *Am J Health Syst Pharm* **56**:1195-1197.
- Rajnarayana K, Reddy MS, Vidyasagar J and Krishna DR (2004) Study on the influence of silymarin pretreatment on metabolism and disposition of metronidazole. *Arzneimittelforschung* **54**:109-113.
- Scott DO and Lunte CE (1993) In vivo microdialysis sampling in the bile, blood, and liver of rats to study the disposition of phenol. *Pharm Res* **10**:335-342.

DMD 14894

Shapiro M and Hyde L (1957) Hyperuricemia due to pyrazinamide *Am J Med* **23**:596-599.

Sheu SY, Lai CH and Chiang HC (1998) Inhibition of xanthine oxidase by purpurogallin and silymarin group. *Anticancer Res* **18**:263-267.

Singh J, Arora A, Garg PK, Thakur VS, Pande JN and Tandon RK (1995) Antituberculosis treatment-induced hepatotoxicity: role of predictive factors. *Postgrad Med J* **71**:359-362.

Snider DE, Graczyk J, Bek E and Rogowski J (1984) Supervised six-months treatment of newly diagnosed pulmonary tuberculosis using isoniazid, rifampin, and pyrazinamide with and without streptomycin. *Am Rev Respir Dis* **130**:1091-1094.

Solangi GA, Zuberi BF, Shaikh S and Shaikh WM (2004) Pyrazinamide induced hyperuricemia in patients taking anti-tuberculous therapy. *J Coll Physicians Surg Pak* **14**:136-138.

Stottmeier KD, Beam RE and Kubica GP (1968) The absorption and excretion of pyrazinamide. I. Preliminary study in laboratory animals and in man. *Am Rev Respir Dis* **98**:70-74.

Tasduq SA, Peerzada K, Koul S, Bhat R and Johri RK (2005) Biochemical manifestations of anti-tuberculosis drugs induced hepatotoxicity and the effect of silymarin. *Hepatol Res* **31**:132-135.

Trnka L, Kuska J and Havel A (1964) Comparison of the antituberculous activity of morphazinamide and pyrazinamide on chronic experimental tuberculosis. I. The antimycobacterial efficacy made in vitro and in vivo. *Chemotherapy* **9**:158-167.

Tsai TH (2001) Pharmacokinetics of pefloxacin and its interaction with cyclosporin A,

DMD 14894

a P-glycoprotein modulator, in rat blood, brain and bile, using simultaneous microdialysis. *Br J Pharmacol* **132**:1310-1316.

Tsai TH, Lee CH and Yeh PH (2001) Effect of P-glycoprotein modulators on the pharmacokinetics of camptothecin using microdialysis. *Br J Pharmacol* **134**:1245-1252.

Valenzuela A, Lagos C, Schmidt K and Videla LA (1985) Silymarin protection against hepatic lipid peroxidation induced by acute ethanol intoxication in the rat. *Biochem Pharmacol* **34**:2209-2212.

van Loenhout-Rooyackers JH, Keyser A, Laheij RJ, Verbeek AL and van der Meer JW (2001) Tuberculous meningitis: is a 6-month treatment regimen sufficient? *Int J Tuberc Lung Dis* **5**:1028-35.

Wagner H, Diesel P and Seitz M (1974) The chemistry and analysis of silymarin from *Silybum marianum* Gaertn. *Arzneimittelforschung* **24**:466-471.

Wagner H, Horhammer L and Munster R (1968) On the chemistry of silymarin (silybin), the active principle of the fruits from *Silybum marianum* (L.) Gaertn. (*Carduus marianus* L.). *Arzneimittelforschung* **18**:688-696.

Weiner IM and Tinker JP (1972) Pharmacology of pyrazinamide: metabolic and renal function studies related to the mechanism of drug-induced urate retention. *J Pharmacol Exp Ther* **180**:411-434.

Yee D, Valiquette C, Pelletier M, Parisien I, Rocher I and Menzies D (2003) Incidence of serious side effects from first-line antituberculosis drugs among patients treated for active tuberculosis. *Am J Respir Crit Care Med* **167**:1472-1477.

Zhao J and Agarwal R (1999) Tissue distribution of silibinin, the major active constituent of silymarin, in mice and its association with enhancement of phase II enzymes: implications in cancer chemoprevention. *Carcinogenesis*

DMD 14894

20:2101-2108.

DMD 14894

Footnotes

Funding for this study was provided in part by research grants (NSC95-2113-M-010-002 from the National Science Council, TCH 95002-62-074; 95004-62-170 from Taipei City Hospital, and V96E2-009 from Taipei Veterans General Hospital) Taiwan.

DMD 14894

Figure legends

Figure 1. Typical chromatograms collected from the rat blood microdialysate 90 min post PZA administration (50 mg kg^{-1} , i.v.) of: (A) standard PA ($10 \text{ } \mu\text{g ml}^{-1}$), PZA ($10 \text{ } \mu\text{g ml}^{-1}$), (B) blank blood dialysate from the microdialysis probe before drug administration, and (C) blood dialysate sample containing PA ($0.45 \text{ } \mu\text{g ml}^{-1}$), PZA ($19.22 \text{ } \mu\text{g ml}^{-1}$). 1: PA, 2:PZA

Figure 2. Typical chromatograms collected from the rat brain microdialysate 40 min post PZA administration (50 mg kg^{-1} , i.v.) of: (A) standard PA ($5 \text{ } \mu\text{g ml}^{-1}$), PZA ($5 \text{ } \mu\text{g ml}^{-1}$), (B) blank brain dialysate from the microdialysis probe before drug administration, and (C) brain dialysate sample containing PZA ($4.26 \text{ } \mu\text{g ml}^{-1}$). 1: PA, 2:PZA

Figure 3. Typical chromatograms collected from the rat bile microdialysate 200 min post PZA administration (50 mg kg^{-1} , i.v.) of: (A) standard PA ($10 \text{ } \mu\text{g ml}^{-1}$), PZA ($10 \text{ } \mu\text{g ml}^{-1}$), (B) blank bile dialysate from the microdialysis probe before drug administration, and (C) bile dialysate sample containing PA ($1.07 \text{ } \mu\text{g ml}^{-1}$), PZA ($12.22 \text{ } \mu\text{g ml}^{-1}$). 1:PA, 2:PZA

Figure 4. Concentration-time profiles for PZA in blood after PZA i.v. administration at a dosage of 50 mg kg^{-1} , and with long-term silibinin exposure and concomitant short-term silibinin exposure groups. Each group of data is represented as means \pm s.e.mean from six individual microdialysis experiments.

Figure 5. Concentration-time profiles for metabolite PA in blood after PZA i.v.

DMD 14894

administration at a dosage of 50 mg kg⁻¹, and with long-term silibinin exposure and concomitant short-term silibinin exposure groups. Each group of data is represented as means \pm s.e.mean from six individual microdialysis experiments.

Figure 6. Concentration-time profiles for PZA in brain after PZA i.v. administration at a dosage of 50 mg kg⁻¹ and with long-term silibinin exposure and concomitant short-term silibinin exposure groups. Each group of data is represented as means \pm s.e.mean from six individual microdialysis experiments.

Figure 7. Concentration-time profiles for PZA in bile after PZA i.v. administration at a dosage of 50 mg kg⁻¹ and with long-term silibinin exposure and concomitant short-term silibinin exposure groups. Each group of data is represented as means \pm s.e.mean from six individual microdialysis experiments.

Figure 8. Concentration-time profiles for metabolite PA in bile after PZA i.v. administration at a dosage of 50 mg kg⁻¹ and with long-term silibinin exposure and concomitant short-term silibinin exposure groups. Each group of data is represented as means \pm s.e.mean from six individual microdialysis experiments.

Figure 9. Concentration-time profiles for PA in blood after PA i.v. administration at a dosage of 30 mg kg⁻¹ and with long-term silibinin exposure and concomitant short-term silibinin exposure groups. Each group of data is represented as means \pm s.e.mean from six individual microdialysis experiments.

DMD 14894

Figure 10. Concentration-time profiles for PA in bile after PA i.v. administration at a dosage of 30 mg kg⁻¹ and with long-term silibinin exposure and concomitant short-term silibinin exposure groups. Each group of data is represented as means ± s.e.mean from six individual microdialysis experiments.

DMD 14894

Table 1

Pharmacokinetic data of PZA in the rat blood, brain and bile, For PZA alone, at a dose of PZA 50 mg kg⁻¹, i.v. was administered. For the PZA + long-term silibinin exposure group, silibinin 100 mg kg⁻¹, p.o. for three consecutive days, on the fourth day PZA 50 mg kg⁻¹, i.v. was administered. For the PZA + concomitant short-term silibinin exposure group, silibinin 30 mg kg⁻¹, i.v. coadministered with PZA 50 mg kg⁻¹, i.v. was administered. Six individual rats were used in each group.

	PZA alone group	PZA + long-term silibinin exposure group	PZA + concomitant short-term silibinin exposure group
PZA			
Blood			
AUC (min µg ml ⁻¹)	19300 ± 3800	18200 ± 4500	20200 ± 2100
Cl (ml kg ⁻¹ min ⁻¹)	2.52 ± 0.8	2.30 ± 0.29	2.12 ± 0.49
t _{1/2} (min)	204 ± 33	189 ± 14	227 ± 79
Cmax (µg ml ⁻¹)	119 ± 31	145 ± 46	144 ± 22
Brain			
AUC (min µg ml ⁻¹)	7900 ± 1700	6900 ± 710	7800 ± 880
t _{1/2} (min)	204 ± 47	165 ± 18	206 ± 38
Cmax (µg ml ⁻¹)	23.7 ± 3.7	27.7 ± 1.5	28.6 ± 2.6
Bile			
AUC (min µg ml ⁻¹)	20500 ± 4200	14900 ± 2300	23900 ± 3600

DMD 14894

$t_{1/2}$ (min)	193 ± 29	123 ± 25	257 ± 45
C_{max} ($\mu\text{g ml}^{-1}$)	91.7 ± 13.8	85.5 ± 10.7	95 ± 9.1
$AUC_{\text{brain}}/AUC_{\text{blood}}$	0.42 ± 0.05	0.44 ± 0.12	0.40 ± 0.08
$AUC_{\text{bile}}/AUC_{\text{blood}}$	1.02 ± 0.16	0.67 ± 0.10	0.96 ± 0.16

Data are expressed as mean \pm s.e.mean. (n=6). * $P < 0.05$ Significantly different from the PZA alone group.

DMD 14894

Table 2

Pharmacokinetic data of the metabolite PA in the rat blood and bile, for PZA alone, at a dose of PZA 50 mg kg⁻¹, i.v. was administered. For the PZA + long-term silibinin exposure group, silibinin 100 mg kg⁻¹, p.o. for three consecutive days, on the fourth day PZA 50 mg kg⁻¹, i.v. was administered. For the PZA + concomitant short-term silibinin exposure group, silibinin 30 mg kg⁻¹, i.v. coadministered with PZA 50 mg kg⁻¹, i.v. was administered. Six individual rats were used in each group.

	PZA alone group	PZA + long-term silibinin exposure group	PZA + concomitant short-term silibinin exposure group
PA			
Blood			
AUC (min µg ml ⁻¹)	212 ± 22	809 ± 69*	568 ± 23*
Bile			
AUC (min µg ml ⁻¹)	527 ± 28	649 ± 29	407 ± 76
AUC _{bile} /AUC _{blood}	2.67 ± 0.63	0.81 ± 0.02*	0.80 ± 0.07*

Data are expressed as mean ± s.e.mean. (n=6). *P<0.05 Significantly different from the PZA alone group.

DMD 14894

Table 3

Pharmacokinetic data of PA in the rat blood and bile, for PA alone, at a dose of PA 30 mg kg⁻¹, i.v. was administered. For the PA + long-term silibinin exposure group, silibinin 100 mg kg⁻¹, p.o. for three consecutive days, on the fourth day PA 30 mg kg⁻¹, i.v. was administered. For the PA + concomitant short-term silibinin exposure group, silibinin 30 mg kg⁻¹, i.v. coadministered with PA 30 mg kg⁻¹, i.v. was administered. Six individual rats were used in each group.

	PA alone group	PA + long-term silibinin exposure group	PA + concomitant short-term silibinin exposure group
PA			
Blood			
AUC (min µg ml ⁻¹)	890 ± 140	3140 ± 300*	3730 ± 380*
Cl (ml kg ⁻¹ min ⁻¹)	0.04 ± 0.08	0.01 ± 0.008	0.01 ± 0.001
t _{1/2} (min)	22 ± 3	27 ± 1*	39 ± 5*
C _{max} (µg ml ⁻¹)	37.2 ± 14.6	97.3 ± 7.6*	119 ± 41*
Bile			
AUC (min µg ml ⁻¹)	3670 ± 190	2830 ± 270*	3610 ± 410
t _{1/2} (min)	35 ± 4	38 ± 9	44 ± 8
C _{max} (µg ml ⁻¹)	81.2 ± 14.1	74 ± 9.1	64 ± 11
AUC _{bile} /AUC _{blood}	3.74 ± 0.41	0.96 ± 0.16*	0.92 ± 0.08*

Data are expressed as mean ± s.e.mean. (n=6). *P<0.05 Significantly different from the PA alone group.

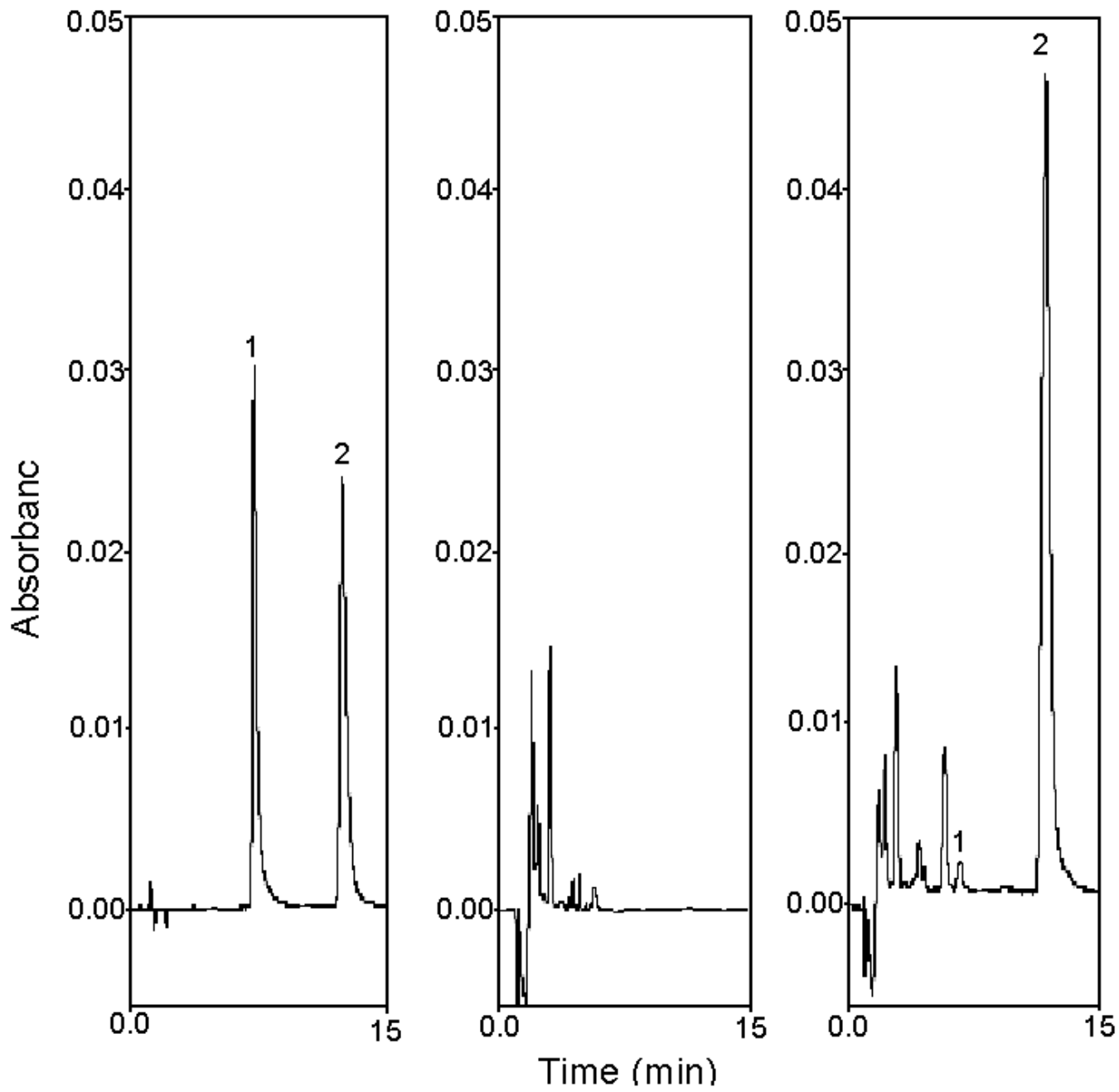


Fig. 1

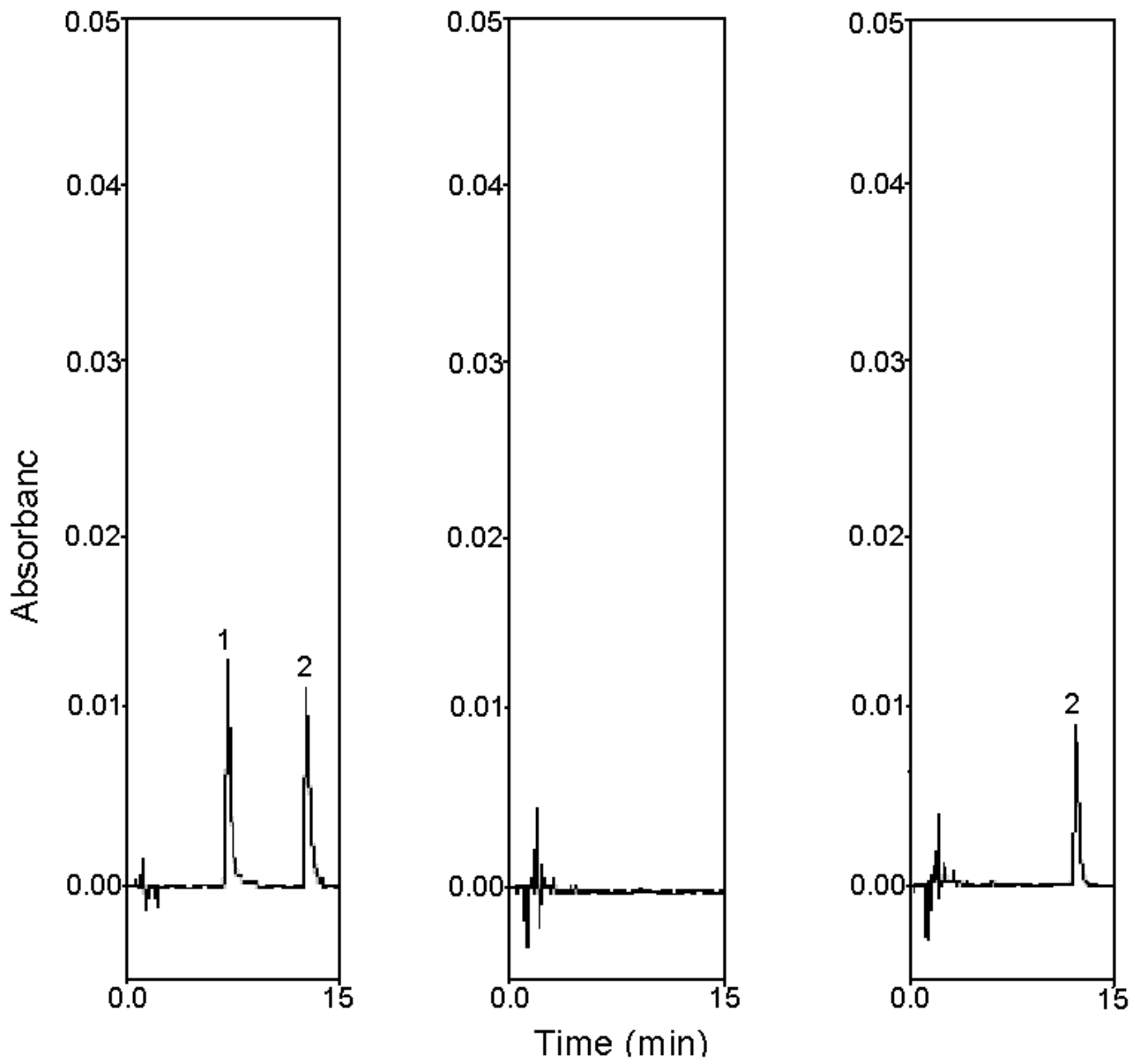


Fig. 2

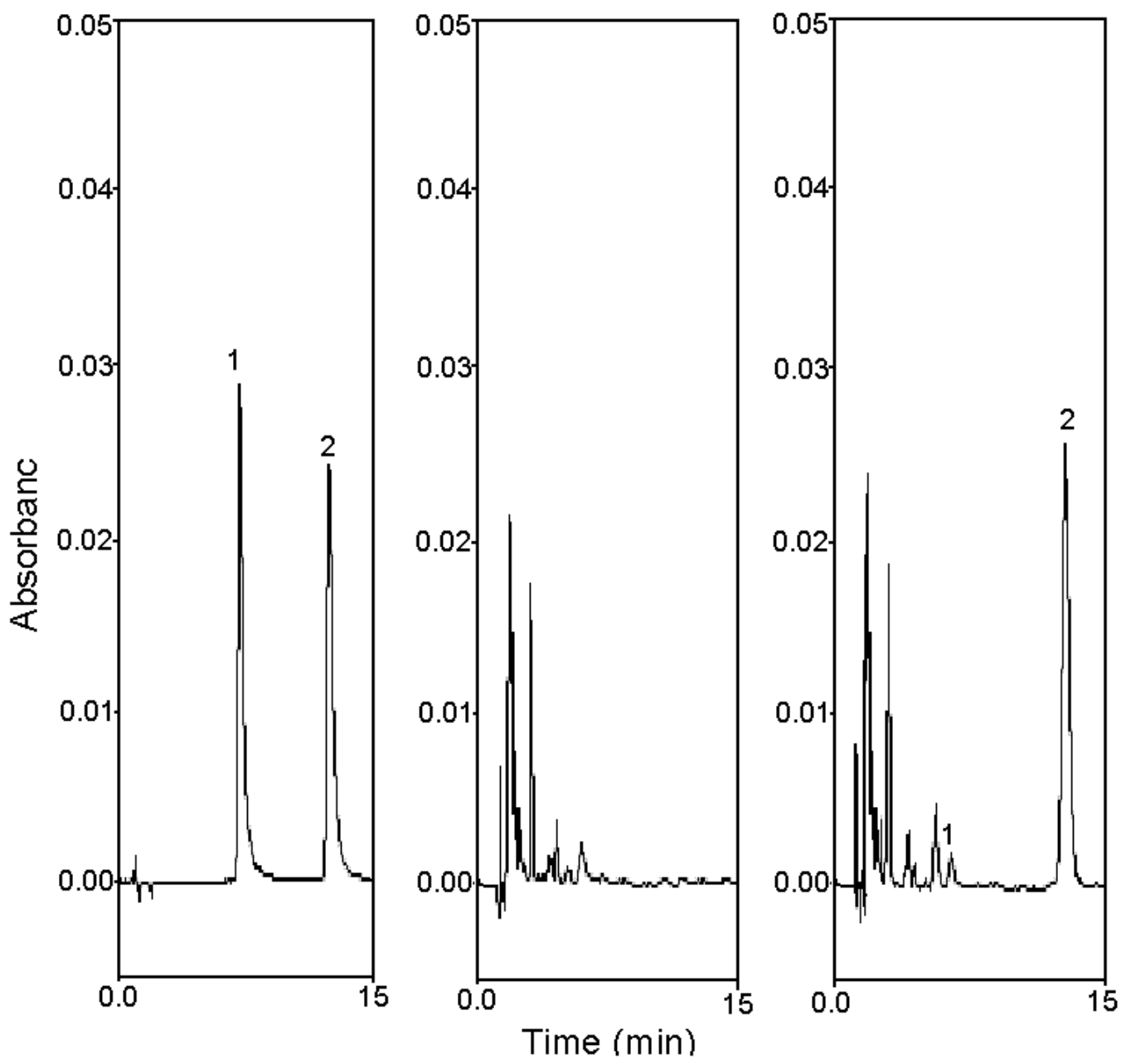


Fig. 3

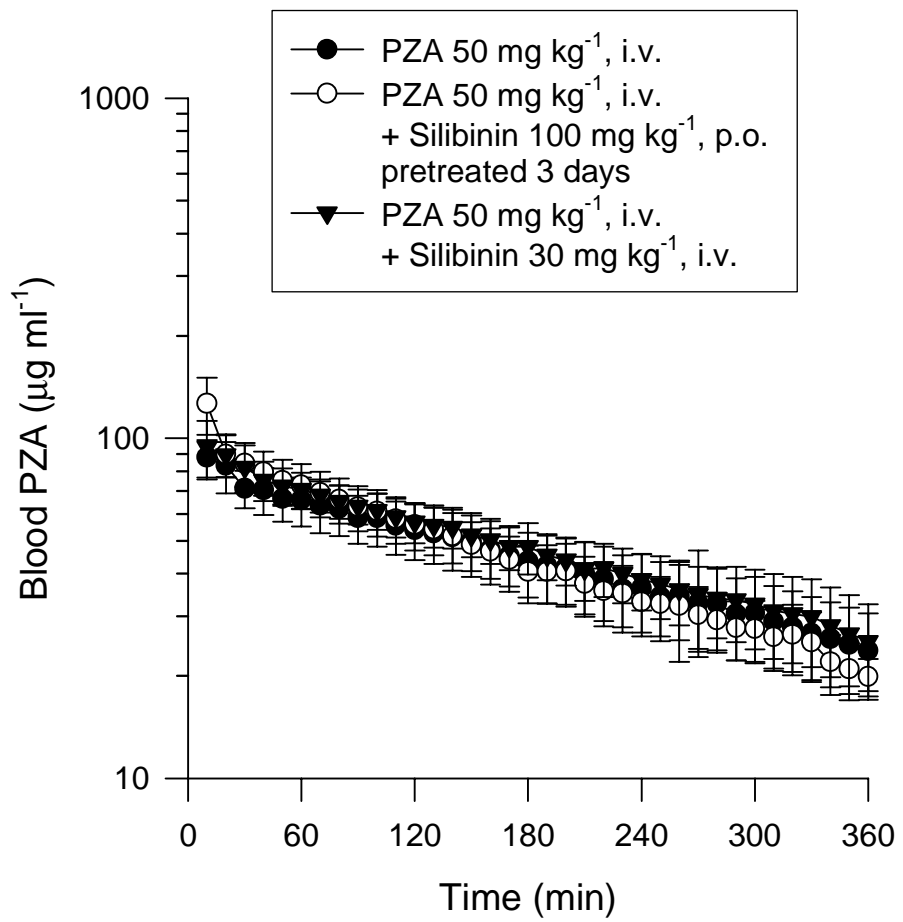


Fig. 4

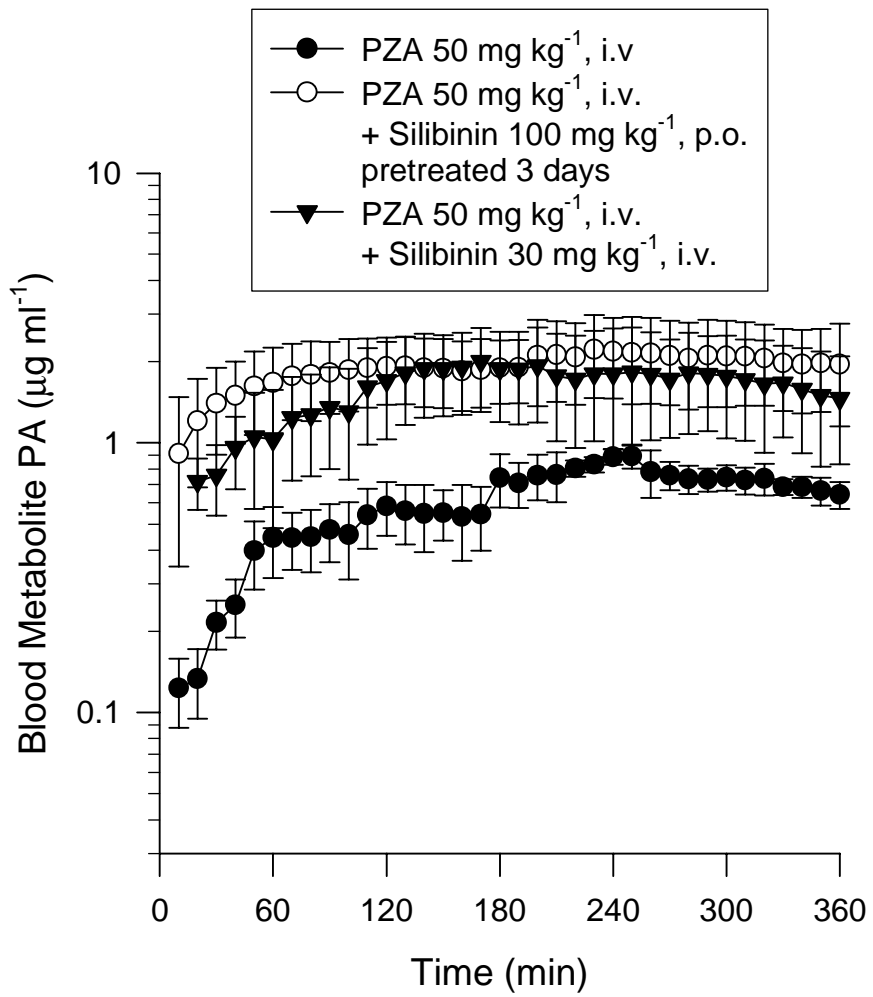


Fig. 5

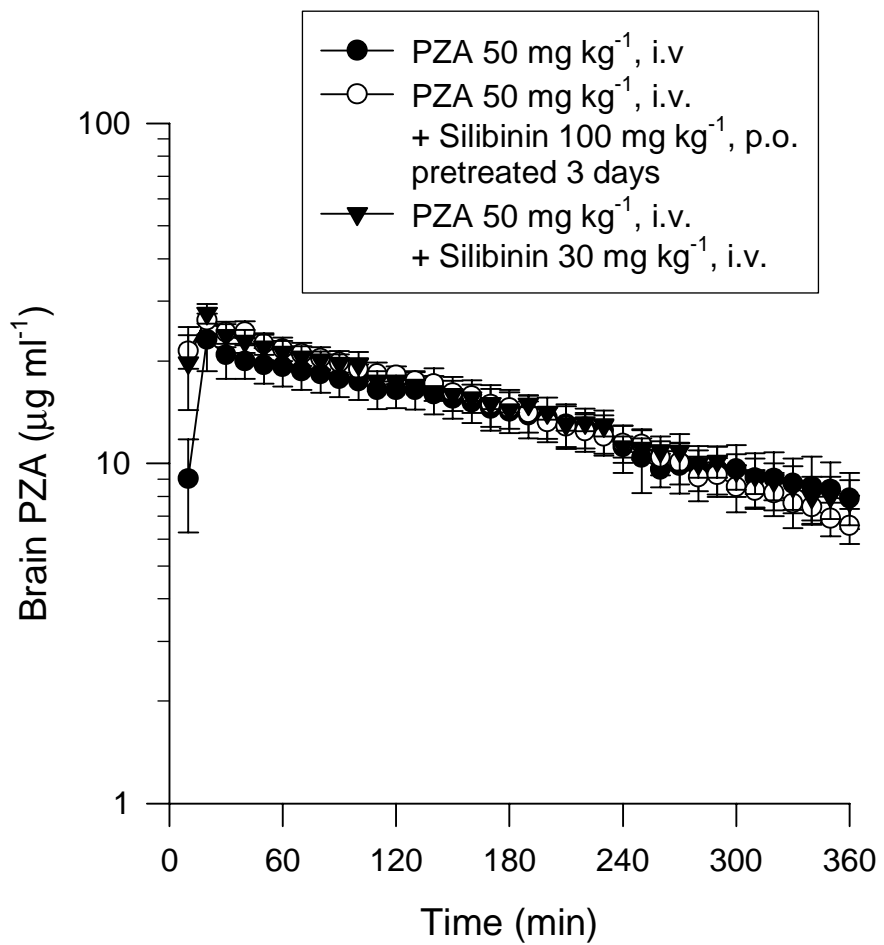


Fig. 6

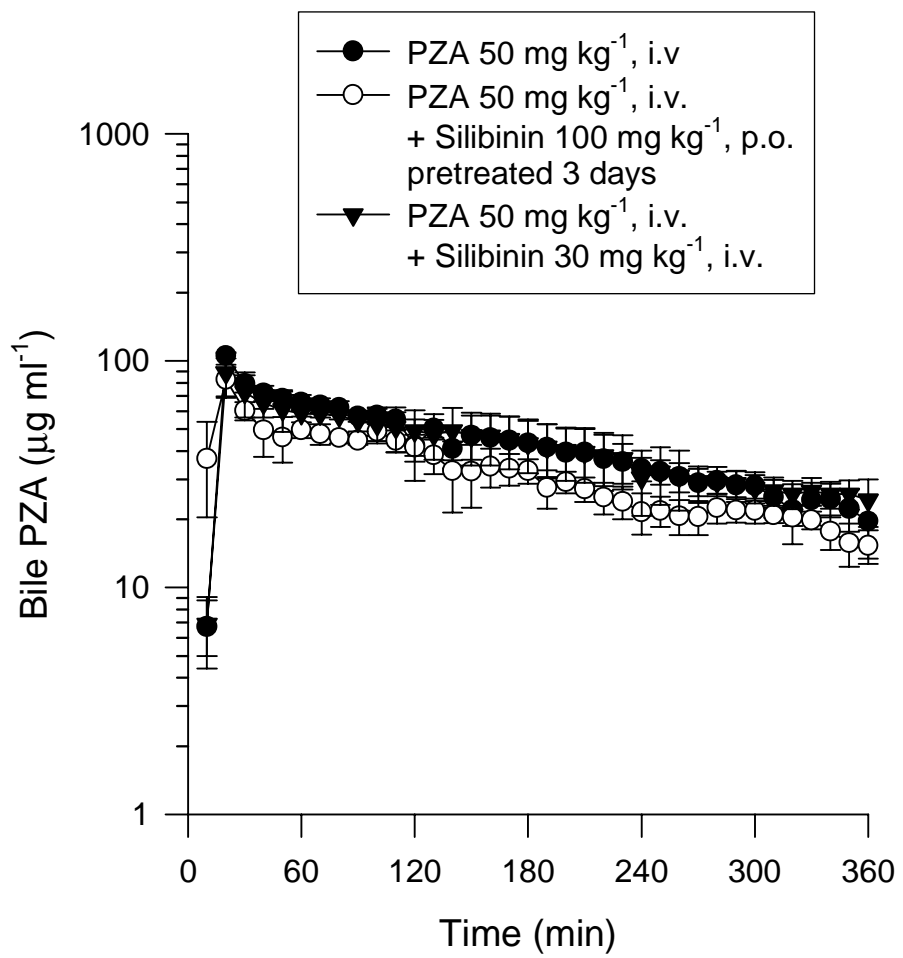


Fig. 7

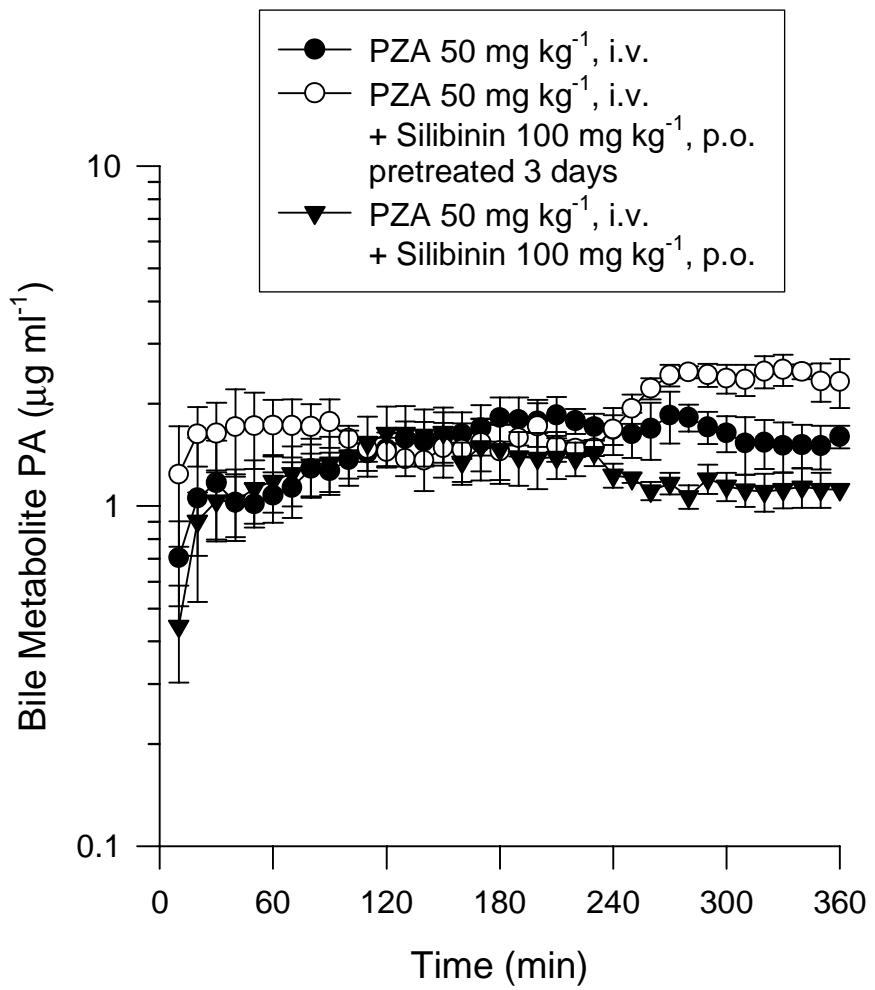


Fig. 8

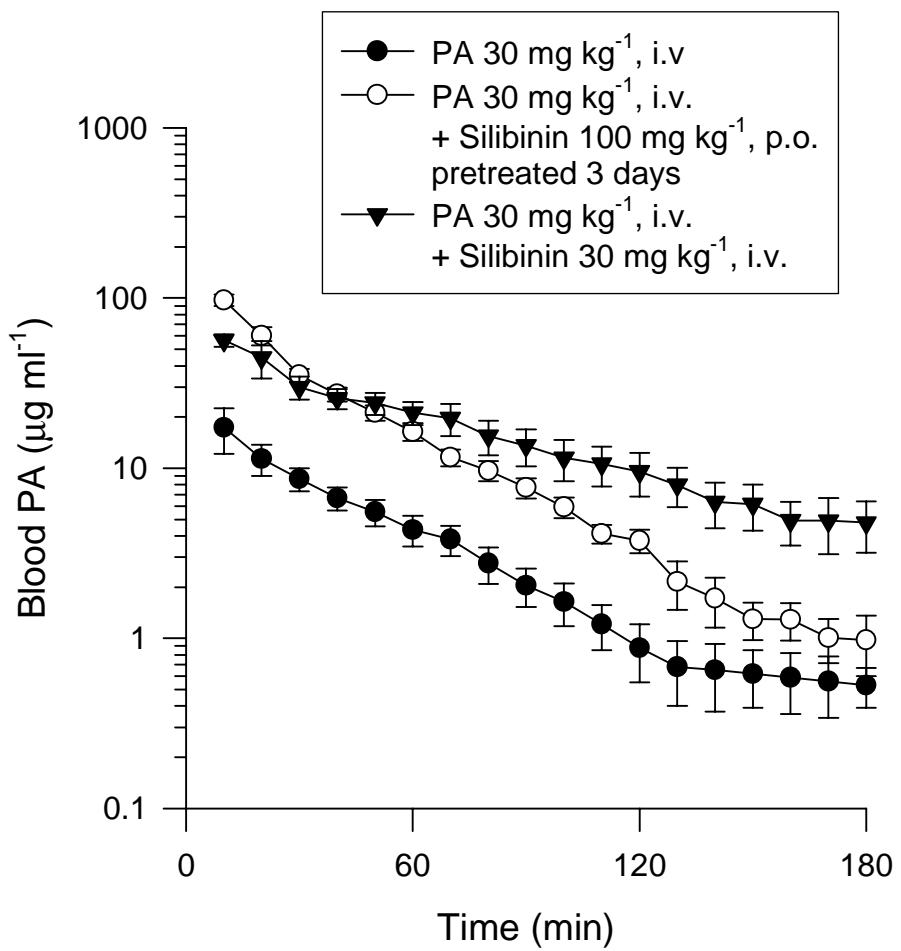


Fig. 9

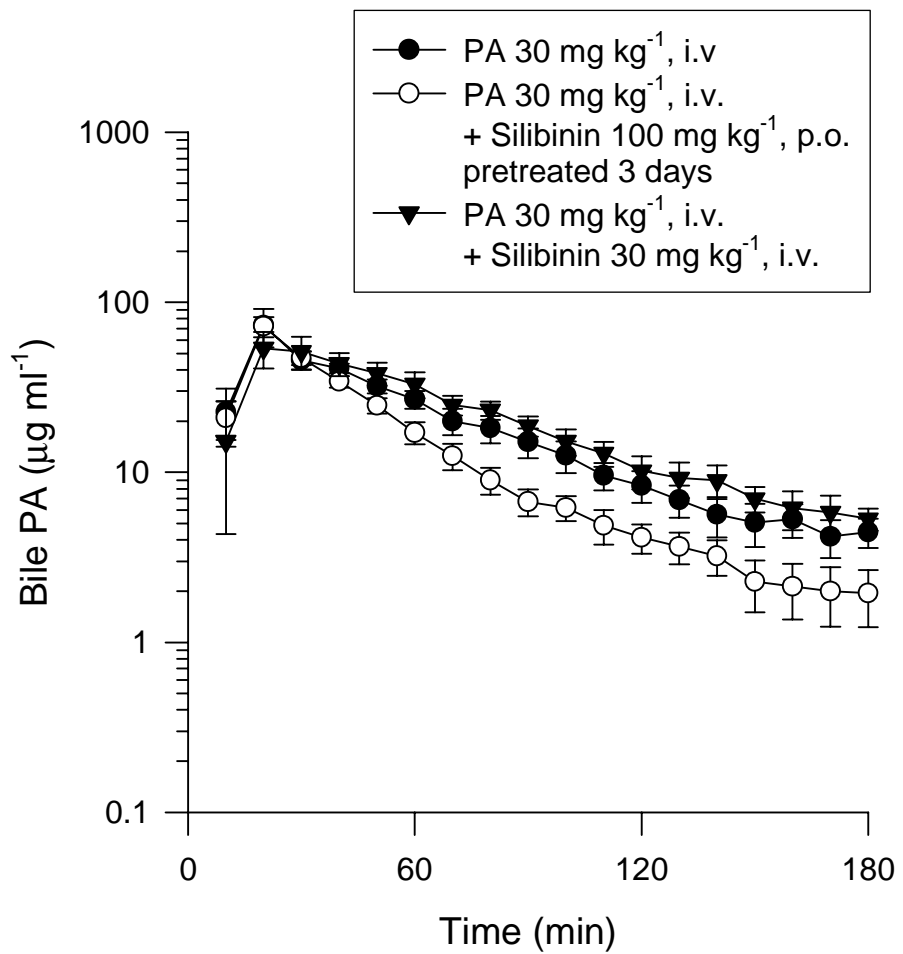


Fig. 10